Resource

TRANSPARENT PROCESS

THE EMBO JOURNAL

Proteomic screening of glutamatergic mouse brain synaptosomes isolated by fluorescence activated sorting

Christoph Biesemann[1], Mads Grønborg[2,10,†], Elisa Luquet[3,4], Sven P Wichert[5,‡], Véronique Bernard[6,7,8], Simon R Bungers[1], Ben Cooper[1], Frédérique Varoqueaux[1], Liyi Li[1], Jennifer A Byrne[9], Henning Urlaub[10,11], Olaf Jahn[12], Nils Brose[1,*] & Etienne Herzog[1,3,4,6,7,8,**]

Abstract

For decades, neuroscientists have used enriched preparations of synaptic particles called synaptosomes to study synapse function. However, the interpretation of corresponding data is problematic as synaptosome preparations contain multiple types of synapses and non-synaptic neuronal and glial contaminants. We established a novel Fluorescence Activated Synaptosome Sorting (FASS) method that substantially improves conventional synaptosome enrichment protocols and enables high-resolution biochemical analyses of specific synapse subpopulations. Employing knock-in mice with fluorescent glutamatergic synapses, we show that FASS isolates intact ultrapure synaptosomes composed of a resealed presynaptic terminal and a postsynaptic density as assessed by light and electron microscopy. FASS synaptosomes contain *bona fide* glutamatergic synapse proteins but are almost devoid of other synapse types and extrasynaptic or glial contaminants. We identified 163 enriched proteins in FASS samples, of which FXYD6 and Tpd52 were validated as new synaptic proteins. FASS purification thus enables high-resolution biochemical analyses of specific synapse subpopulations in health and disease.

Keywords Fluorescence Activated Synaptosome Sorting; proteomics; subcellular fractionation; synaptosome; vesicular glutamate transporter
Subject Categories Neuroscience; Methods & Resources

DOI 10.1002/embj.201386120 | Received 28 June 2013 | Revised 10 November 2013 | Accepted 18 November 2013
EMBO Journal (2014) 33, 157–170

Introduction

The mammalian brain contains a complex network of neurons that communicate via many different types of synapses, as well as glial cells and blood vessels. To reduce this complexity for experimental purposes, numerous approaches were developed to purify isolated synaptic particles, which were termed 'synaptosomes' by Victor Whittaker. Synaptosomes are functional synaptic connections consisting of a resealed presynaptic compartment and part of the postsynaptic element (Whittaker *et al*, 1964), and a wealth of knowledge about synapse structure, composition, and function has been gained from studies on synaptosomes (Whittaker, 1993; Bai & Witzmann, 2007; Morciano *et al*, 2009).

A major limitation of conventional synaptosome preparations is that they contain a mixture of synapse types (49.1% of all particles) and many neuronal and non-neuronal contaminations (50.9% of all particles; Cotman & Matthews, 1971; Henn *et al*, 1976; Dodd *et al*, 1981). This heterogeneity confounds the interpretation of synaptosome-derived data and the identification of new synaptic proteins by proteomics (Abul-Husn & Devi, 2006; Tribl *et al*, 2006).

1 Department of Molecular Neurobiology, Max Planck Institute of Experimental Medicine, Göttingen, Germany
2 Department of Neurobiology, Max Planck Institute of Biophysical Chemistry, Göttingen, Germany
3 CNRS, IINS, UMR 5297, Bordeaux, France
4 University of Bordeaux, IINS, UMR 5297, Bordeaux, France
5 Gene Expression Group, Department of Neurogenetics, Max Planck Institute of Experimental Medicine, Göttingen, Germany
6 INSERM U952, Université Pierre et Marie Curie, Paris, France
7 CNRS UMR 7224, Paris, France
8 Université Pierre et Marie Curie (UPMC) Paris 06, PMSNC, Paris, France
9 Molecular Oncology Laboratory, Children's Cancer Research Unit, Kids Research Institute, Westmead, NSW, Australia
10 Bioanalytical Mass Spectrometry, Max Planck Institute for Biophysical Chemistry, Göttingen, Germany
11 Bioanalytics, Department of Clinical Chemistry, University Medical Center Göttingen, Göttingen, Germany
12 Proteomics Group, Max Planck Institute of Experimental Medicine, Göttingen, Germany
*Corresponding author. Tel: +49 551 3899 725; Fax: +49 551 3899 715; E-mail: brose@em.mpg.de
**Corresponding author. Tel: +33 5 57 57 57 48; Fax: +33 5 57 57 40 82; E-mail: etienne.herzog@u-bordeaux2.fr
†Department of Beta Cell Regeneration, Hagedorn Research Institute, Gentofte, Denmark
‡Department of Psychiatry and Psychotherapy, Ludwig-Maximilians-University Munich, Munich, Germany

Isolation of unfixed, unpermeabilized, and functional subpopulations of synaptosomes has been attempted using immunoaffinity purification. However, the use of intracellular antigens for these purposes raised major concerns with regard to the specificity of the corresponding preparations that were never properly addressed (Docherty *et al*, 1987), and the very limited number of tractable synapse surface markers has prevented the improvement of immunopurification approaches. Alternative approaches involved flow cytometry-based analyses and sorting of synaptosomes that had been aldehyde-fixed, in some cases permeabilized, and immunolabelled (Wolf & Kapatos, 1989a,b; Gylys *et al*, 2004; Sokolow *et al*, 2012). Key problems arising from such studies are that synaptosomes are by an order of magnitude smaller than an average cell, to which the FACS instruments are calibrated, and cannot be expanded after purification. Consequently, sorting of synaptosomes requires particle detection methods that do not depend on light scattering, and long sorting times are needed to accumulate sufficient material for further analysis. So far, the exact nature, purity, and morphology of alleged synaptosomal particles analysed or prepared by flow cytometry have never been validated systematically, and the quality of corresponding synaptosome preparations is questionable.

Glutamate is the main excitatory neurotransmitter in the central nervous system of vertebrates. It operates in most neuronal circuits, and the glutamatergic system is involved in almost all physiological and pathophysiological brain processes. Consequently, the molecular basis of glutamatergic synaptic transmission has received massive attention. Vesicular glutamate transporters (VGLUTs) are the only specific markers for glutamatergic synapses (Fremeau *et al*, 2004; Takamori, 2006), but due to their intracellular localization on synaptic vesicles (SV) they cannot be used as targets for synaptosome immunoisolation. To circumvent this problem, we generated a knock-in mouse line that expresses a fully functional VGLUT1^{VENUS} protein instead of wild-type (WT) VGLUT1 (Herzog *et al*, 2011) so that all synapses that normally contain VGLUT1 are fluorescently labeled by VGLUT1^{VENUS}. Using these mice, we established the first protocol for FACS isolation of intact glutamatergic synaptosomes. This Fluorescence Activated Synaptosome Sorting (FASS) protocol represents a novel approach to enrich specific synapses to near homogeneity. Purified material can be studied by immunofluorescence and electron microscopy, Western blotting, and proteomic techniques. Further, FASS allows high-resolution separation of synaptic and extrasynaptic components of neurons and the identification of novel components of VGLUT1-containing synapses.

Results

Fluorescence Activated Synaptosome Sorting (FASS)

We used VGLUT1^{VENUS} knock-in mice to prepare fluorescent glutamatergic synaptosomes with a conventional sucrose density centrifugation protocol (Whittaker, 1959; S-synaptosomes). S-synaptosomes were subjected to FASS, and sedimented onto glass coverslips for immunofluorescence imaging, or concentrated on polycarbonate filters for Western blotting, mass spectrometry (MS), or electron microscopy (Fig 1). S-synaptosomes from mouse forebrain are expected to contain 50% synaptic particles, of which some 80% are expected to be VGLUT1-containing synaptosomes. Hence S-synaptosomes contain about 30–40% particles that represent VGLUT1^{VENUS}-positive synaptosomes. As a consequence, a two to threefold enrichement of VGLUT1^{VENUS} synaptosomes from S-synaptosomes is expected to yield nearly pure VGLUT1^{VENUS} synaptosomes.

Flow analysis and sorting of particles require the adequate triggering of measurements when particles cross the analysis volume. To optimize the triggering of synaptosome detection, we bulk-stained all membranes in S-synaptosomes using FM4-64 (Fig 2A) and thresholded to avoid triggering by buffer background noise (Fig 2B). To identify and sort VGLUT1^{VENUS} synaptosomes among FM4-64-detected particles, we first gated for size using the 'small size' gate that rejects larger debris and aggregated particles. Then, a gate for VGLUT1^{VENUS} fluorescence (sorted fluorescence) allowed to discriminate particles brighter than autofluorescence measured in WT synaptosomes (Fig 2C and D). On average, VGLUT1^{VENUS} synaptosome preparations contained 14.3 ± 1.5% small and fluorescent particles eligible for sorting (Fig 2D1). Flow-analyzed samples after sorting displayed a global shift towards higher fluorescence signals (from 23.1 ± 2.3% total fluorescent particles pre-sorting, to 51.7 ± 1.1% post-sorting, Fig 2E and H) that was even stronger with small fluorescent particles (from 14.3 ± 1.5% to 49.3 ± 1.2%; Fig 2D1 and G1). As we eliminated aggregates, sorted particles distributed homogeneously in the small size gate (96.9 ± 0.22; Fig 2G). To more accurately estimate the abundance of the respective subpopulations of particles in our samples (Fig 2), we fitted the flow cytometry data (four experiments) with a multiple normal distribution component model. Our analysis predicts that 18 ± 5.2% of the unsorted particles and 64.8 ± 1.9% of the sorted particles are positively fluorescent, which matches a 3.6-fold absolute enrichment and a 8.4-fold relative enrichment of fluorescent versus non-fluorescent particles during sorting (supplementary Fig S1).

Validation of FASS sample quality

Our FASS protocol was expected to purify intact VGLUT1^{VENUS}-positive synaptosomes, and hence to co-enrich proteins present in VGLUT1^{VENUS}-containing synapses while depleting proteins present in other particles of the S-synaptosome preparation. To test this, we determined the relative co-enrichment factors (CF; Fig 3A–C) of several proteins to VGLUT1^{VENUS} levels by Western blotting.

The SV markers Synaptophysin, Synapsin-1, VAMP2 and Rab3a co-enriched with VGLUT1 in FASS samples (CF 1.01 ± 0.1, 0.86 ± 0.15, 1.5 ± 0.18, 0.97 ± 0.37 respectively; Fig 3A and B) as did the SV endocytosis markers EndophilinA1 (a soluble interactor of VGLUT1; De Gois *et al*, 2006; Vinatier *et al*, 2006; Voglmaier *et al*, 2006), Dynamin1 and Clathrin LC (CF 1.4 ± 0.03; 0.72 ± 0.09; 0.58 ± 0.04 respectively), and the mitochondrial voltage-dependent anion-selective channel (Shoshan-Barmatz *et al*, 2010; VDAC; CF of 1.11 ± 0.07), which is expected as most synapses contain mitochondria (Shepherd & Harris, 1998). Non-synaptic glial contaminants are present in S-synaptosome fractions, but the microglial ionized calcium binding adapter molecule 1 (Imai *et al*, 1996; IBA1; CF 0.23), the astrocytic plasma membrane glutamate transporter (Pines *et al*, 1992; EAAT2/GLT1; CF 0.18 ± 0.06), and the oligodendrocytic proteolipid protein (Greer & Lees, 2002; PLP; not detectable) were strongly depleted from the FASS samples (Fig 3A and B). As synapses of all neurotransmitter phenotypes are present in S-synaptosomes,

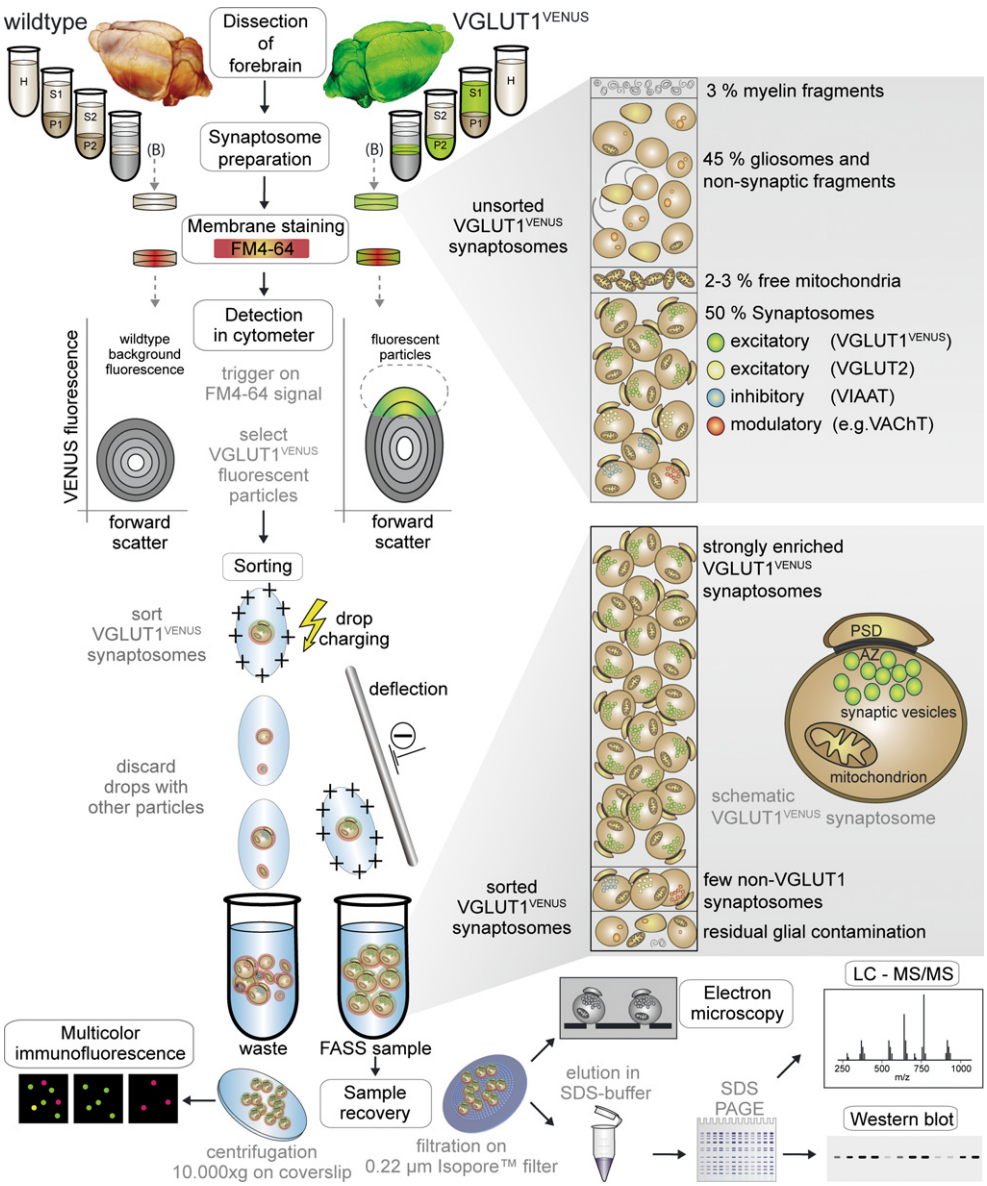

Figure 1. Overview of the FASS protocol.
Wild-type and VGLUT1^{VENUS} forebrains were dissected, homogenized, and subjected to subcellular fractionation yielding the synaptosome fraction (B). H, homogenate; P1, pellet 1; S1, supernatant 1; P2, pellet 2; S2, supernatant 2 (for details see Materials and Methods). All particles of the synaptosomal fraction were then stained with FM4-64, which was used to trigger detection of particles in the sorter. Wild-type samples were used to determine the level of autofluorescence in the VENUS channel. Only fluorescent particles brighter than autofluorescence were sorted in the VGLUT1^{VENUS} samples. Drops that contained contaminating particles were discarded as waste. The FASS sample was collected by filtration or centrifugation, depending on the subsequent analysis. Intact VGLUT1^{VENUS}-positive synaptosomes were composed of a fragment of the postsynapse, a presynaptic active zone, SVs, and mitochondria. FASS samples were analyzed by immunofluorescence or electron microscopy, Western blotting, and proteomic techniques. The higher purity of FASS-purified VGLUT1^{VENUS}-positive synaptosomes is illustrated schematically.

we tested FASS samples for synaptic markers that are absent from VGLUT1 synapses (Masson *et al*, 1999; Fremeau *et al*, 2004). We found that FASS strongly depleted the SV transporters VAChT (CF 0.12 ± 0.05), VIAAT (CF 0.28 ± 0.05), and VGLUT2 (CF 0.30 ± 0.07) relative to VGLUT1^{VENUS} (Fig 3A and C), and we confirmed depletion of VIAAT using quantitative immunofluorescence staining (Fig 4D and E).

The quality of the FASS preparation was further assessed by electron microscopy. VGLUT1^{VENUS}-selective and all particles control sorts were sampled (Fig 2F and G), filtered onto polycarbonate membranes, and systematically imaged and quantified. Intact synaptosomes (Fig 3F and H) and non-synaptic profiles (debris; Fig 3G) were identified and delineated. As compared to control samples, synaptosomes in VGLUT1^{VENUS} FASS samples were twice as frequent and covered 4.87 times more surface relative to debris (Fig 3I). As control samples contain all types of synaptosomes this result still underestimates the real enrichment in VGLUT1 synapses by FASS (Fig 3A and C).

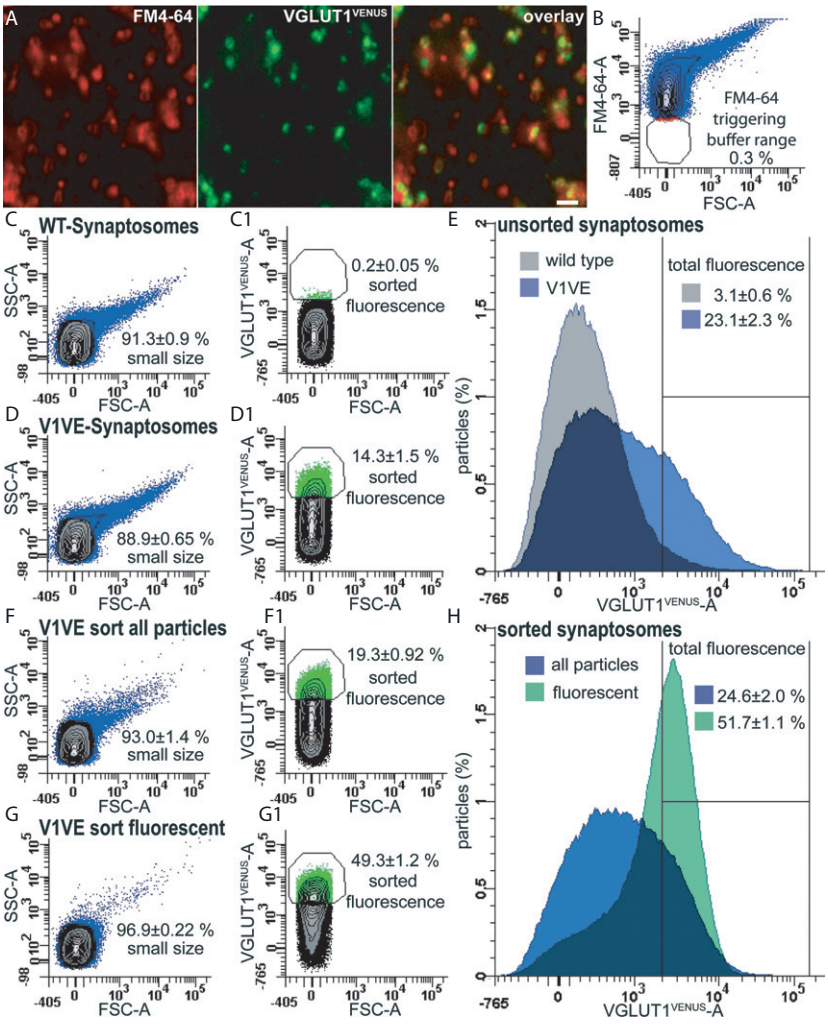

Figure 2. Analysis and gating of VGLUT1^{VENUS}-positive synaptosomes. Representative flow-cytometry data. Each plot shows 100,000 events.

A FM4-64 lipophilic styryl dye labeling of synaptosomes to trigger the detection of microparticles. Confocal microscopy images of FM4-64-stained VGLUT1^{VENUS} S-synaptosomes. Note the more homogeneous size range of VGLUT1^{venus} particles. Scale bar, 2 μm.

B Fluorescence triggering of FM4-64-stained synaptosomal particles with a threshold set to block out buffer background.

C, C1 Analysis of WT synaptosomes determines the level of autofluorescence in the VENUS channel.

D, D1 Analysis of VGLUT1^{VENUS} samples. Only particles of the combined 'small size' and 'sorted fluorescence' gates were sorted and reanalyzed.

E Comparison of WT and VGLUT1^{VENUS} distributions of fluorescent signals. The fluorescence threshold for the 'total fluorescence' gate is the same as for the 'sorted fluorescence' gate.

F, F1 Reanalysis of a non-selective sort of all particles.

G, G1 Reanalysis of sorted fluorescent VGLUT1^{VENUS}-positive particles of small size. Note the homogeneous light scattering of this particle population and the significant shift toward high VENUS fluorescence signals.

H Comparison of the distributions of fluorescence signals of all particles versus fluorescent particles.

Data information: In the contour plots (C–G), contour lines mark differences of 10% probability, and outliers with a probability of <5% are plotted as dots. For each gate the percentages given are the average of four independent experiments. +/− errors indicate the average deviation from the mean.

Subsynaptic protein localization by FASS

We next tested if the previously reported synapse-specific distribution of various synaptic proteins can be confirmed by FASS. Consistent with published evidence (Bajjalieh *et al*, 1994), the SV glycoprotein 2A (SV2A; CF 0.68 ± 0.05) was significantly less co-enriched with VGLUT1^{VENUS} as compared to its homologue SV2B (CF 1.02 ± 0.05; Fig 4A and B). In accord with previously published immunoelectron microscopy data (Yamada *et al*, 1999), we found the presynaptic SNARE complex regulator Complexin2 (Cpx-2; CF 1.09 ± 0.11) to be enriched to a similar extent as VGLUT1^{VENUS}, while the homologue Cpx-1 (0.54 ± 0.06) was depleted (Fig 4A and B). Synaptosome-associated proteins of 25 and 23 kDa (SNAP25 and SNAP23) are thought to be differentially localized at VGLUT1 synapses (Bragina *et al*, 2007). However, we found a strong co-enrichment of both SNAP25 (CF 1.45 ± 0.07) and

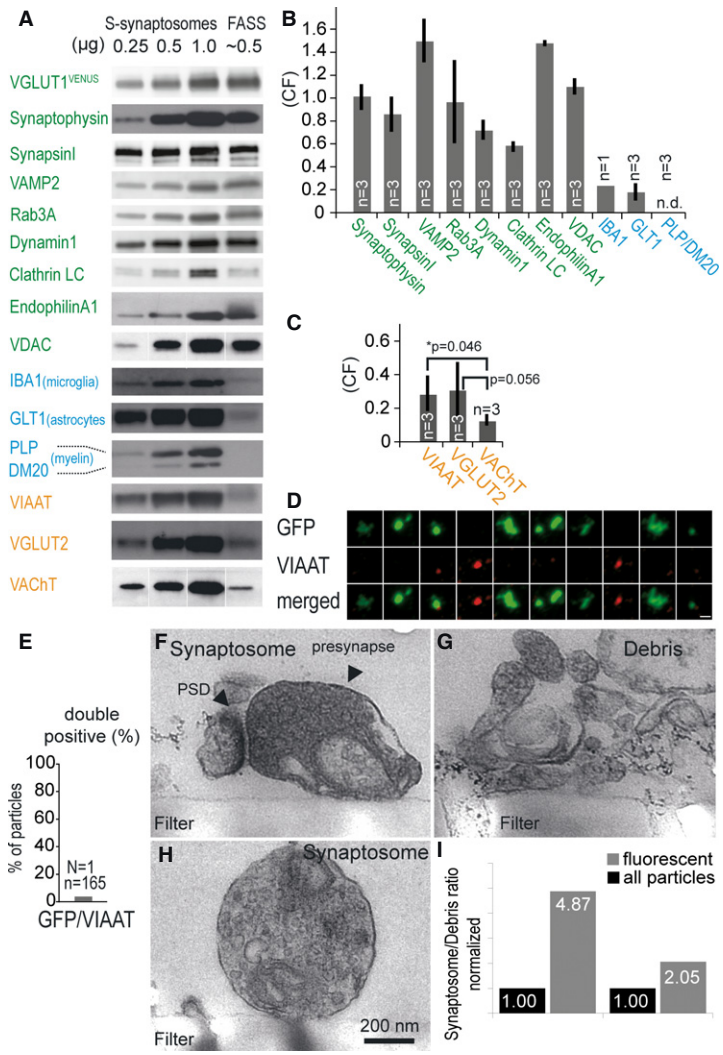

Figure 3. Characterization of FASS VGLUT1^{VENUS}-positive synaptosomes.

A Representative Western blot profiles of S-synaptosomes (0.25–1 µg) and FASS VGLUT1^{VENUS} synaptosomes (~0.5 µg). In some cases, lanes from the same blot were rearranged for presentation (white separators). VGLUT1/2, vesicular glutamate transporter 1/2; VDAC, voltage-dependent anion channel; IBA1, ionized calcium binding adaptor molecule 1; GLT1, glutamate transporter 1; PLP, myelin proteolipid protein; DM20, isoform DM20 of myelin proteolipid protein; VIAAT, vesicular inhibitory amino acid transporter; VAChT, vesicular acetylcholine transporter; VAMP2, vesicle-associated membrane protein 2.

B, C Quantification of Western blots series shown in (A). Data are represented as the co-enrichment factor (CF) ± s.e.m. for each protein, relative to the enrichment of VGLUT1^{VENUS} in the sorted versus unsorted sample. Asterisks indicate significant pairwise differences in a one-sided *t*-test ($P < 0.05$). *n*, number of independent experiments.

D Representative immunofluorescence micrographs of sorted VGLUT1^{VENUS}-positive synaptosomes stained for VGLUT1^{VENUS} (anti-GFP; note the 0.5–1.5 µm expected size range) and VIAAT. Scale bar, 1 µm.

E Quantification of VGLUT1^{VENUS}/VIAAT double positive particles (see D). One hundred and sixty-five GFP-positive particles from one FASS experiment ($N = 1$; $n = 165$).

F–I A non-selective sort of all particles was compared to FASS-purified VGLUT1^{VENUS}-positive synaptosomes by ultrastructural analysis on the collection filters (see Fig 2D–F). Electron micrographs allowed the identification of synaptosomes (F and H) or material classified collectively as debris (G). Filters were imaged and analyzed systematically by an observer blinded to the experimental condition. Synaptosomal and debris structures were manually outlined and quantified using ImageJ (I). Note that the number of synaptic profiles is doubled and their relative surface area is increased 4.87-fold in the FASS-purified sample.

SNAP23 (CF 1.07 ± 0.28) with VGLUT1^{VENUS} (Fig 4A and B). This contradicts the notion that SNAP23 and VGLUT1 are segregated to different synapses. In addition, SNAP47, thought to be partially localized at synapses (Holt *et al*, 2006), was enriched in FASS samples to a similar extent (CF 1.08 ± 0.13) as VGLUT1 (Fig 4A and B).

The presence of postsynaptic elements in synaptosomal profiles was already observed but not quantified in the pioneering synaptosome studies (Gray & Whittaker, 1962). We immunolabeled FASS synaptosomes for the post-synaptic density marker PSD95 and found that 78.4 ± 3.14% of VGLUT1^{VENUS}-positive particles were also

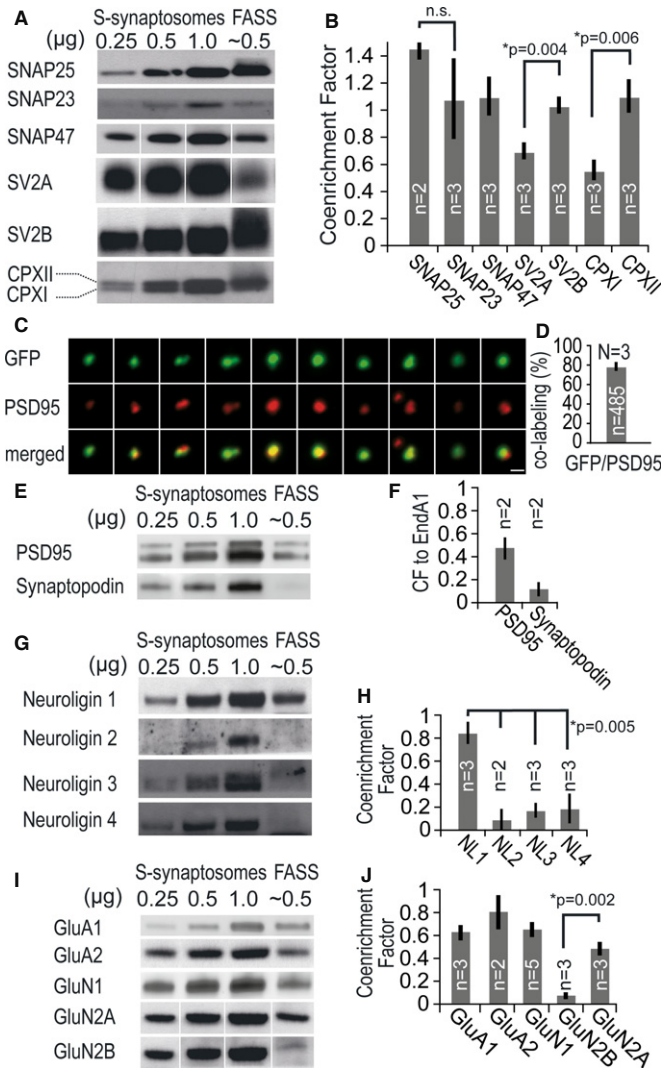

Figure 4. High-resolution delineation of the synaptic compartment in VGLUT1^{venus} FASS purified synaptosomes.

A, B Analysis of the co-enrichment of several presynaptic protein isoforms. SNAP23/25/47, synaptosomal associated protein of 23/25/47 kDa; SV2A/B, synaptic vesicle protein 2A/B; n.s., not significant. *n*, number of independent experiments.

C Representative immunofluorescence micrographs of sorted VGLUT1^{VENUS}-positive synaptosomes stained for VGLUT1^{VENUS} (anti-GFP) and PSD95. VGLUT1^{VENUS} is usually associated with the staining of postsynaptic PSD95. Scale bar, 1 µm.

D Quantification of PSD95/VGLUT1^{venus} apposition in 485 GFP-positive particles from three independent FASS experiments (see C; n = 485; N = 3).

E, F Analysis of PSD95 and Synaptopodin1 enrichments by Western blot (E) and corresponding quantifications (F).

G, H Analysis of co-enrichment of the four Neuroligin isoforms (NL1-4) in the sorted VGLUT1^{VENUS}-positive synaptosomes by Western blot (G) and the corresponding quantification (H). *n*, number of independent experiments.

I, J Analysis of co-enrichment of several subunits of postsynaptic glutamate receptors in the sorted VGLUT1^{VENUS}-positive synaptosomes by Western blot (I) and the corresponding quantification (J). White separators indicate when lanes from the same blot were rearranged for presentation. *n*, number of independent experiments.

positive for PSD95 (N = 3; n = 485; Fig 4C and D). Additionally we performed Western blot analysis of PSD95 and the spine neck marker Synaptopodin1. While PSD95 was coenriched in FASS synaptosomes, Synaptopodin1 was strongly depleted upon VGLUT1^{VENUS} particle sorting (CF relative to EndophilinA1 0.45 ± 0.11 and 0.12 ± 0.05 respectively; Fig 4E and F). We then performed Western blot analysis on a subset of postsynaptic proteins. The postsynaptic Neuroligins (NL1-4 in rodents) regulate synapse maturation and function (Krueger *et al*, 2012). We found that NL1 was enriched (CF 0.84 ± 0.09) in VGLUT1^{VENUS} FASS samples whereas NL2, NL3, and NL4 were largely depleted (CF 0.08 ± 0.08 for NL2; CF 0.16 ± 0.05 for NL3; CF 0.18 ± 0.12 for NL4; Fig 4G and H). Accordingly, NL1 is the main NL isoform at glutamatergic synapses while NL2 and NL4 are specifically localized to inhibitory synapses (Krueger *et al*, 2012). The synapse specificity of NL3 is only known for the cerebellum, where it is present at subsets of different synapse types (Baudouin *et al*, 2012).

Pharmacological and morphological (Hippenmeyer *et al*, 2004) but not biochemical data (Okabe, 2007) indicate that GluN2A-containing NMDA-type glutamate receptors are concentrated in the PSDs of adult forebrain synapses while GluN2B-containing receptors function extrasynaptically. We found GluA1 (CF 0.63 ± 017), GluA2 (CF 0.8 ± 1.58), GluN1 (CF 0.65 ± 0.06), and GluN2A (CF 0.48 ± 0.06) in FASS samples while GluN2B was significantly depleted (CF 0.07 ± 0.03; Fig 4G and H), which supports the notion that GluN2B is localized extrasynaptically (Fig 4I and J).

Screening proteins of VGLUT1-containing synapses by FASS

The FASS VGLUT1^{VENUS} synaptosomes seem to be highly depleted of typical S-synaptosome contaminants. To further assess this, we performed systematic comparative analyses of the protein composition of sorted and unsorted synaptosome samples using MS-based protein identification and semi-quantitative spectral counting. Samples were separated by one-dimensional SDS-PAGE, tryptically digested in the gel, and analyzed by nanoLC-MS/MS (Fig 5A). Using Mascot as a search engine, 2,212 and 2,044 proteins were identified in S-synaptosomes (supplementary Table S1) and in the FASS sample (supplementary Table S2), respectively. A subset of 1,075 proteins were analyzed for enrichment or depletion during the FASS procedure by stringent semi-quantitative spectral counting (scaffold2 software; Proteome Software, Inc., Portland, OR, USA; supplementary Table S3). Of these, 163 proteins were found to be ≥ 2-fold enriched in FASS samples whereas 343 proteins were depleted ≥ 2-fold (Fig 5A).

VGLUT1, Synaptophysin, VAMP2, EndophilinA1, SNAP25, SV2A, SV2B, and PSD95 were ≥ 2-fold enriched in the FASS sample, while NL2, NL3, Synaptopodin and PLP were depleted by ≥ 2-fold (Fig 5B). Synapsin-1 (1.66), Rab3a (1.66), Dynamin1 (1.25), ClathrinLC (1), SNAP47 (1.1), Complexin-2 (1.43), VDAC (1.66), and GluN1 (1.25) were enriched in the FASS sample by ≤ 2-fold, while Complexin-1 (0.91), GluN2B (0.91), GluA1 (0.83), GluA2 (0.91), and GLT-1 (0.83) were ≤ 2-fold depleted (Fig 5B). For 23 of these 25 proteins, spectral counting trends were in agreement with western-blot quantification (Figs 3–5).

We compared our proteomic data to mRNA expression profiles of astrocytes, oligodendrocytes, and neurons (Cahoy *et al*, 2008). For most ≥ 2-fold enriched or depleted proteins, cell type-specific mRNA expression data were available so that we compared and clustered

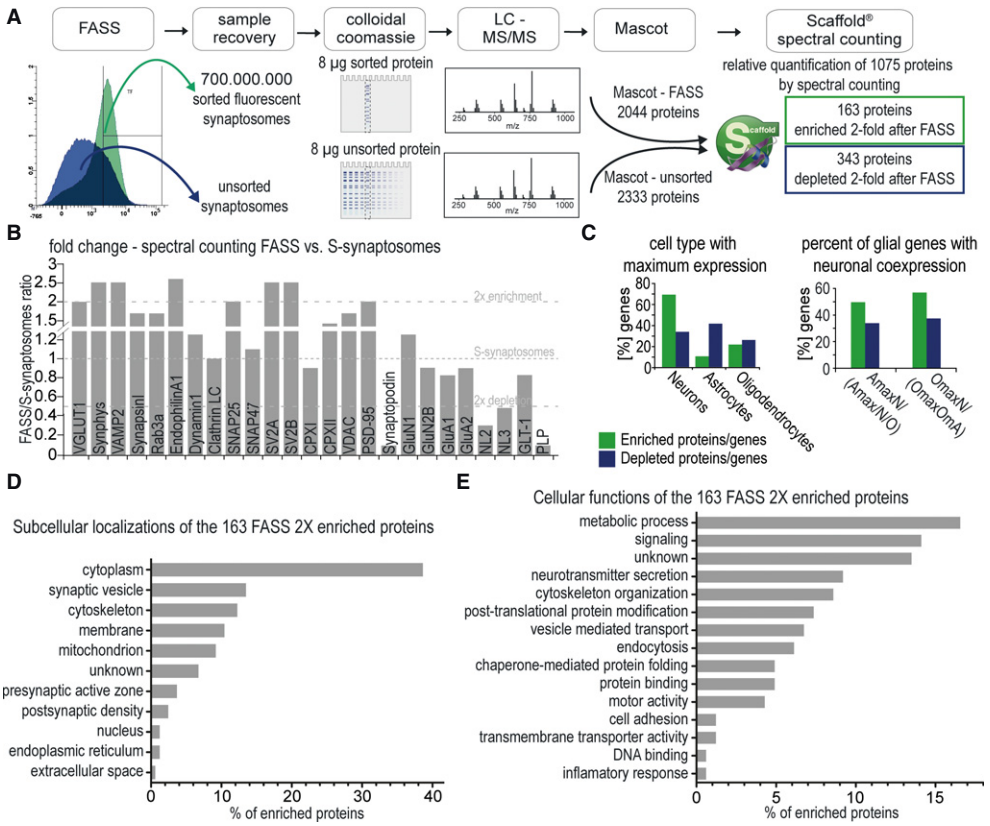

Figure 5. Comparative proteomic analysis of S-synaptosomes and FASS purified VGLUT1^{VENUS}-positive synaptosomes.

A Following SDS-PAGE and tryptic digestion, proteins of both samples were analyzed by high-resolution tandem MS. The enrichment and depletion of proteins in sorted versus unsorted synaptosomes were determined by spectral counting using Scaffold. Of 1,075 quantified proteins, 163 were enriched by a factor of two or more, while 343 were depleted by a factor of two or more (listed in supplementary Tables S1–S3).

B Fold change of protein spectral counts between the FASS-purified and S-synaptosomes for selected targets that were also analyzed by Western blotting (see Figs 3 and 4). Fold depletion is plotted as negative values and fold enrichment as positive values.

C Spectral countings were compared with mRNA expression data of neurons, oligodendrocytes, and astrocytes (Cahoy *et al*, 2008). Relative contributions of genes with maximal expression in neurons (Nmax, NmaxA, NmaxO), astrocytes (Amax, AmaxN, AmaxO) and oligodendrocytes (Omax, OmaxN, OmaxA) are plotted as percentages of differentially expressed genes (see supplementary Fig S2 for detailed clusters). Among astrocyte and oligodendrocyte genes, percentages of genes classified to have relatively high expression in neurons are also plotted (e.g. AmaxN/(Amax+AmaxN+AmaxO); OmaxN/(Omax+OmaxN+OmaxA)).

D Subcellular localizations of the 163 proteins enriched twofold or more in FASS samples.

E Cellular functions of the 163 proteins enriched twofold or more in FASS samples.

them accordingly (supplementary Fig S2 and Table S3). The percentage of proteins with maximal mRNA expression in neurons was twofold higher in the FASS-enriched fraction (68.7%, including typical excitatory synapse components) than in the depleted fraction (33.3%, including typical inhibitory neuron markers; Fig 5C and Fig S2). In contrast, protein products of genes with maximal mRNA expression in astrocytes were fourfold more abundant in the FASS-depleted fraction (41 versus 10.1%). In addition, the FASS-enriched proteins included a twofold larger fraction of proteins originating from genes with relatively high co-expression in neurons (Fig 5C).

Finally the 163 proteins that we found to be significantly enriched in our VGLUT1^{venus} FASS samples were classified according to their known localization and function in cells using gene ontology terms (GO). General GO categories were preferred over specific ones to extract global information on the sample composition (supplementary Table S4 and Fig 5D and E). Proteins of the major synaptic compartments and functions were identified, with the notable exception of glutamate receptors, which were enriched less than twofold in the FASS samples. Twenty-two proteins of unknown cellular function were identified, while others are of known function or subcellular localization but were not anticipated as synaptic proteins (supplementary Table S4 and Fig 5D and E). Of the latter, FXYD6 and Tpd52 were studied further.

FXYD6 and Tpd52 are novel components of VGLUT1-containing synapses

Indeed, FXYD6 was enriched in FASS-sorted VGLUT1^{VENUS}-containing synaptosomes according to spectral counting, and its mRNA is preferentially present in neurons (Cahoy *et al*, 2008; supplementary Fig S2A and Table S3). FXYD integral membrane proteins (FXYD1-7) bind to and modulate the function of Na^+/K^+-ATPase (Garty & Karlish, 2006; Geering, 2006). FXYD6 was detected in all brain regions, with strongest expression in the forebrain. Upon subcellular

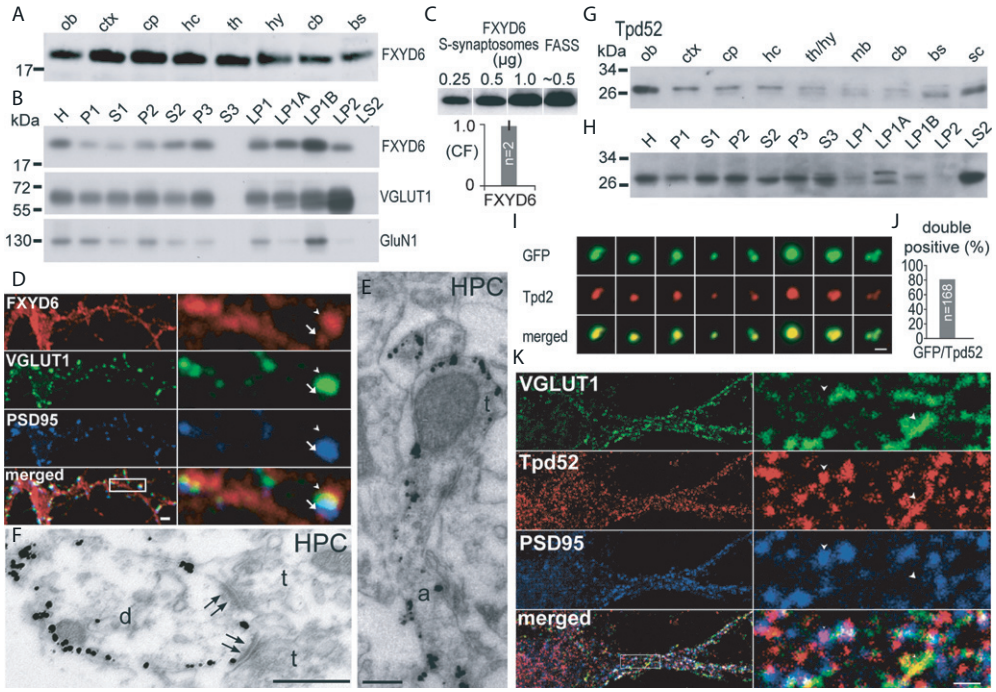

Figure 6. FXYD6 and Tpd52 are localized to VGLUT1-positive synapses.

A Regional distribution of FXYD6 in adult mouse brain homogenates. ob, olfactory bulb; ctx, cerebral cortex; cp, caudate-putamen; hc, hippocampus; th, thalamus; hy, hypothalamus; cb, cerebellum; bs, brainstem.

B FXYD6, VGLUT1, GluN1 distribution in subcellular fractions of mouse brain. Note that FXYD6 is markedly enriched in the synaptic plasma membrane fraction LP1B. H,homogenate; P1, nuclear pellet; S1, supernatant 1; P2, crude synaptosomes; S2, supernatant 2; P3, microsomal fraction; S3, somatic soluble fraction; LP1, lysed P2 pellet 1; LP1A, myelin-rich light membrane fraction; LP1B, synaptic plasma membrane fraction; LP2, crude SVs; LS2, soluble synaptic fraction.

C FXYD6 enrichment in sorted VGLUT1^{VENUS} synaptosomes by Western blot analysis. The average CF of 0.97 for FXYD6 with VGLUT1 in FASS-purified synaptosomes indicates a high rate of copurification of the two markers. The error bar indicates the s.e.m. *n*, independent experiments.

D Immunofluorescence of FXYD6 (red), VGLUT1 (green), and PSD95 (blue) in primary cultured hippocampal neurons. Scale bars, 2 µm in overviews and 0.4 µm for enlarged images.

E, F Pre-embedding immunoelectron microscopy of ultrathin sections of mouse hippocampus using the anti-FXYD6 antibody. HPC, hippocampus; t, terminal; a, axon; d, dendrite. Double arrows mark synaptic contacts. Scale bars, 0.5 µm (E and F).

G Western blot analysis of the distribution of Tpd52 in homogenates of different brain regions of adult mice. ob, olfactory bulb; ctx, cerebral cortex; cp, caudate-putamen; hc, hippocampus; th/hy, thalamus and hypothalamus; mb, mid brain including colliculi, substantia nigra and ventral tegmental area; cb, cerebellum, bs, brainstem; sc, spinal cord.

H Western blot analysis of Tpd52 in subcellular fractions of mouse brain. Samples used here are identical to those employed in (B).

I Representative immunofluorescence micrographs of sorted VGLUT1^{VENUS}-positive synaptosomes stained for VGLUT1^{VENUS} (anti-GFP) and Tpd52. Scale bar, 1 µm.

J Quantification of VGLUT1^{VENUS}/Tpd52 double positive particles (see C). A total of 168 GFP-positive particles from one FASS experiment were analyzed (n = 168; N = 1).

K Triple immunofluorescence staining for VGLUT1 (green), Tpd52 (red), and PSD95 (blue) in cultured primary hippocampal neurons (DIV22). Arrowheads mark examples of co-localization of Tpd52 with VGLUT1 or PSD95. Scale bar, 1 µm in enlarged images and 6 µm for overviews.

fractionation, FXYD6 was strongly enriched in the synaptic plasma membrane fraction (LP1B; Fig 6A and B), and following FASS, it co-enriched with VGLUT1^{VENUS} (CF of 0.97; Fig 6C). FXYD6 Immunofluorescence in cultured hippocampal neurons revealed a somatodendritic and axonal localization, with intense punctate staining in direct apposition to VGLUT1 and PSD95 (Fig 6D). FXYD6 was also identified at VGLUT2 synapses and in a small minority of GABAergic neurons but not in astrocytes (see supplementary Fig S3A–C). Ultrastructural pre-embedding, silver-enhanced immunogold labeling confirms a localization of FXYD6 at presynaptic, axonal, and dendritic plasma membranes in hippocampus and striatum (Fig 6E and F and supplementary Fig S3D).

Like FXYD6, Tpd52 was enriched in sorted VGLUT1^{VENUS}-positive synaptosomes according to spectral counting (supplementary Fig S2A and Table S3). Tpd52 belongs to a family of proteins implicated in vesicle trafficking and secretory processes (Boutros *et al*, 2004), and interacts with MAL2 (Wilson *et al*, 2001), a specific component of VGLUT1-containing SVs (Grønborg *et al*, 2010). It is expressed strongly in olfactory bulb and spinal cord, and moderately in cortex, caudate-putamen, hippocampus, and brainstem (Fig 6G). Upon subcellular fractionation, Tpd52 was strongly enriched in the synaptic cytosol fraction (LS2; Fig 6H), 80% of FASS-sorted VGLUT1^{VENUS}-positive synaptosomes also contained Tpd52 (Fig 6I and J), and immunofluorescence staining showed that Tpd52 often co-localizes with both VGLUT1, PSD95 and MAP2 (Fig 6K and supplementary Fig S4B), but not with GABAergic compartements (supplementary Fig S4A).

Although our biochemcial, FASS, immunostaining and EM data on FXYD6 and Tpd52 are consistent and strongly indicate that FXYD6 and Tpd52 are localised to synaptic plasma membranes and to soluble synaptic compartments, respectively, further studies using for example corresponding knock-out mice as controls are necessary to unequivocally confirm our conclusions.

Discussion

We report here the enrichment of VGLUT1-containing synapses to unprecedented purity through fluorescence activated sorting of synaptosomes from VGLUT1^{VENUS} knock-in mice. Using FASS, we obtained very specific biochemical insights into the cellular and subcellular localization of several synaptic proteins. A comparative screen of proteins contained in S-synaptosomes and in VGLUT1^{VENUS} FASS isolated synaptosomes identified 163 proteins that are specifically enriched in FASS-sorted synaptosomes. Among these were multiple proteins that had not previously been described at synapses, inluding FXYD6 and Tpd52, which we identified and characterized as new components of VGLUT1-containing synapses.

Single synaptosomes can only be isolated by FM4-64-triggered sorting

Prior to the present study, the characteristics of synaptosome preparations generated by flow cytometry had been analyzed only cursorily, and methods to validate sample quality were limited. We therefore developed a filtration procedure to recover FASS-purified synaptosomes for western blotting, proteomics, and electron microscopy, and a centrifugation protocol for immunofluorescence staining (Fig 1).

Synaptosome detection in the FACS was reported to be possible using FSC triggering (Wolf & Kapatos, 1989a,b; Gylys *et al*, 2004). We show that detection of the whole population of synaptosomal particles requires the establishment of VENUS-independent FM4-64 fluorescence staining for FSC-independent triggering of particle detection (Fig 2A and B). Only under these conditions did we isolate VGLUT1^{VENUS}-positive particles that could be fully validated using FACS-independent methods. Our immunofluorescence and electron microscopy analyses of FASS-sorted VGLUT1^{VENUS}-positive synaptosomes showed single particles of the expected size range of 0.5 to 2 μm (Figs 2 and 3D and I). VGLUT1 synaptosomes are estimated to represent roughly 30–40% of particles in S-synaptosome preparations from murine forebrain, VGLUT1^{venus} enriched two- to three-fold during sorting as assessed by Western blot and MS analyses. Further, FASS strongly depleted VIAAT (inhibitory synapse marker), VAChT (cholinergic synapse marker), PLP (myelin marker), GLT1 (astrocyte marker), IBA1 (microglia marker), and VGLUT2 (marker for glutamatergic synapses that mostly do not contain VGLUT1) from the purified VGLUT1^{VENUS}-positive synaptosomes (Fig 3A–E). Finally, FM4-64-triggered purification isolated particles containing proteins of all functional elements expected to be present in VGLUT1-containing synaptosomes (see Figs 3–5 and supplementary Tables).

Taken together, these findings demonstrate that glutamatergic synaptosomes isolated by the VGLUT1^{VENUS}-based FASS protocol with FM triggering are enriched to near homogeneity, and most contaminants that are found in conventional synaptosome preparations are strongly depleted.

High-resolution fractionation of presynaptic and postsynaptic proteins by FASS

To date, our FASS protocol is the only method to detect differential synaptic distributions of proteins using biochemical synaptosome preparations (see Fig 4). For example, we confirmed the differential synaptic localization of VGLUTs, SV2s, and Cpxs (but not of SNAPs) that had previously been demonstrated using histochemistry (Bajjalieh *et al*, 1994; Takahashi *et al*, 1995; Yamada *et al*, 1999; Fremeau *et al*, 2004; Bragina *et al*, 2007; Brose, 2008; Südhof & Rothman, 2009; Grønborg *et al*, 2010). As reported previously, synaptosomes may contain a fragment of the postsynapse (Whittaker, 1993), and our immunofluorescence staining experiments show that at least 80% of FASS-purified glutamatergic synaptosomes have a PSD attached (Fig 4C and D). Moreover, we found that PSD95 is coenriched by FASS as assessed by immunostaining, Western blot and MS analyses, while the spine neck marker Synaptopodin1 is massively depleted (Figs 4E,H and 5B). We can thus define VGLUT1 synaptosomes as particles containing presynapses and the post-synaptic density membrane, but not whole spines. Postsynaptic cell adhesion proteins of the Neuroligin family (NL1-4) are synapse type-specific regulators of synaptic maturation and function (Krueger *et al*, 2012). We confirmed the expected enrichment of the glutamatergic NL1 (Song *et al*, 1999) and the expected depletion of the GABAergic NL2 isoform (Varoqueaux *et al*, 2004) in FASS-purified glutamatergic synaptosomes. Further, we found that both NL3 and NL4 are depleted from VGLUT1^{VENUS}-positive synaptosomes (Fig 4G and H). Accordingly, NL4 was reported to be associated with inhibitory synapses in many brain regions (Hoon *et al*, 2011). NL3 seems to be present at both types of synapses in the cerebellum (Baudouin *et al*, 2012), and our findings indicate that NL3 is largely absent from forebrain glutamatergic synapses *in vivo*.

Identification of the synaptic neurotransmitter receptor complement by FASS

The neurotransmitter receptor complement defines many of the functional features of a given synapse. FASS purified VGLUT1^{VENUS}-positive synaptosomes contained GluN2A but not GluN2B as assessed by Western blotting (Fig 4I and J). Thus, a large fraction of GluN2B in the conventional synaptosomes is present in particles distinct from VGLUT1-containing synaptosomes. This segregation of NMDA receptor subunits, which had previously escaped detection with biochemical methods, corroborates pharmacological, electrophysiological and single molecule tracking data indicating that the GluN2B subunit of the NMDA receptor is preferentially localized to extrasynaptic sites while GluN2A is predominantly synaptic (Hippenmeyer *et al*, 2004; Thomas *et al*, 2006; Bard & Groc, 2011). Likely, neuronal extrasynaptic particles containing Synaptopodin1, which are removed by FASS, may also contain extrasynaptic receptors like GluN2B.

Our data on the synaptic versus extrasynaptic segregation of GluN2A and GluN2B indicate that conventional synaptosome

samples contain many non-synaptic compartements, including detergent-insoluble scaffolds of extrasynaptic NMDA-receptors (Al-Hallaq *et al*, 2001; Gardoni *et al*, 2006; Milnerwood *et al*, 2010). On aggregate, the FASS protocol presented here provides a promising biochemical approach for the analysis of synaptic versus extrasynaptic protein pools in physiology and pathology.

Proteomic analysis of FASS purified VGLUT1^{VENUS}-containing synaptosomes

Based on the FASS method, we provide the first proteomic profiling of a neurotransmitter system specific subset of intact synaptosomes and its comparison with conventionally enriched bulk forebrain synaptosomes. We identified over 2,000 proteins in the FASS sorted sample (Fig 5A, supplementary Table S2). 1075 proteins identified with high confidence were quantified using spectral counting. Among the 434 proteins displaying a preferential partitioning with VGLUT1^{VENUS}-positive synaptosomes, 163 were enriched $\geq$ 2-fold (supplementary Tables S3 and S4). Among these, we found many well-characterized components of glutamatergic synapses (Chua *et al*, 2010). Three hundred and forty-three proteins that were depleted $\geq$ 2-fold in the FASS sample were either of non-synaptic neuronal or glial origin or specific to other neurotransmitter systems (supplementary Table S3). The reliability of our semi-quantitative approach is supported by the finding that the trends of enrichment or depletion of 23 proteins were replicated by Western blotting while only two quantifications mismatched (Fig 5B). The comparison of our proteomic screen with cell type-specific mRNA expression data (Cahoy *et al*, 2008) shows that the mRNAs of proteins enriched by FASS are largely expressed in a neuron-specific manner, while the mRNAs of many depleted proteins showed glia-specific expression. Many components of inhibitory neurons and synapses, whose mRNAs are neuron-specific, such as $GABA_A$-receptor subunits, NL2, and Calretinin, were found among the proteins depleted by FASS (Fig 5B and C and supplementary Fig S2). Classification of the 163 enriched proteins according to cell location and function categories shows that most cellular compartments and functions expected to be relevant to synapses are represented in the set of enriched proteins. Among these, the 22 proteins with unknown function and proteins that are not expected to enrich at glutamatergic synapses based on current knowledge are of particular interest.

FASS-purified VGLUT1^{VENUS}-positive synaptosomes are thus among the most reliable sources for mass-spectrometric identification of novel synaptic proteins.

FXYD6 and Tpd52 as novel components of VGLUT1-containing excitatory synapses

We found FXYD6 and Tpd52 to be strongly enriched in FASS samples as assessed by spectral counting, although they had not previously been implicated in glutamatergic or general synapse function.

Proteins of the FXYD family (FXYD1-7 in mammals) regulate Na^+/K^+-ATPase function (Garty & Karlish, 2006). We show here for the first time that FXYD6 is enriched at pre- and postsynaptic plasma membranes of VGLUT1-positive synapses (Fig 6). Further analysis revealed that FXYD6 is also present in VGLUT2 and inhibitory hippocampal neurons but hardly or not at all in co-cultured GFAP-positive astrocytes (supplementary Fig S3). FXYD6 has been studied most intensively in the inner ear, where its expression levels during development correlate with the establishment of the ion-homeostasis necessary for proper auditory signaling (Delprat *et al*, 2007). FXYD6 decreases the apparent $K_{1/2}(Na^+)$ of $\alpha1\beta1$ Na^+/K^+-ATPases and increases the $K_{1/2}(Na^+)$ of $\alpha1\beta2$ isozymes (Delprat *et al*, 2007). In addition, FXYD6 was previously found in the membranes of somata and dendrites of auditory neurons and neurons in cortex, hippocampus, and cerebellum (Yamaguchi *et al*, 2001; Kadowaki *et al*, 2004; Delprat *et al*, 2007), where it may play a role in the control of cell excitability.

Tpd52 (tumor protein D52) was originaly identified because of its upregulation in human breast cancer and cancer cell lines (Byrne *et al*, 1996), and multiple lines of evidence have implicated Tpd52 in secretory processes (Parente *et al*, 1996; Groblewski *et al*, 1999; Chew *et al*, 2008). Using immunofluorescence staining, we confirmed the presence of Tpd52 in most VGLUT1^{VENUS} synaptosomes (Fig 6I and J). For the first time, Tpd52 was shown to be a soluble component of pre- and postsynaptic compartments (Fig 6K). In line with our findings, *Tpd52* mRNA and protein were detected in the brain and in neurons (Chew *et al*, 2008; Oldham *et al*, 2008), and yeast two-hybrid assays identified Tpd52 protein family members as binding partners of MAL2 (Wilson *et al*, 2001), a specific component of VGLUT1-containing SVs (Grønborg *et al*, 2010).

On aggregate, our data provide a first proof-of-principle for the use of FASS to identify new synaptic proteins with a potential regulatory role in glutamatergic neurotransmission. FXYD6 may regulate the synaptic and perisynaptic membrane potential while Tpd52 may participate in pre- and postsynaptic membrane trafficking.

Future applications of FASS

The FASS method described here represents an important methodological advance over conventional synaptosome fractionation approaches (Whittaker, 1993). It allows to determine the synaptic localization of candidate proteins at unprecedented biochemical resolution, and to screen for new components of glutamatergic synapses. Our new method and the corresponding dataset nicely complement previously published methods and data on the proteomic composition of synaptic vesicles (Takamori *et al*, 2006; Burré & Volknandt, 2007), active zones (Morciano *et al*, 2009; Boyken *et al*, 2013) and postsynaptic densties (Cheng *et al*, 2006; Collins *et al*, 2006). In this regard, a major asset of our approach is that it allows for the stringent enrichment of cytosolic presynaptic proteins, which has not been done so far. Future thorough comparisons of the respective methods and datasets will lead to a more detailed understanding of the synaptic protein complement and its subsynaptic compartmentalization. In the context of mouse lines modeling brain diseases, the combination of the FASS method with modern isotope labeling-based or label-free quantitative proteomic approaches provides the possibility to systematically determine disease-relevant aberrations of glutamatergic synapse proteomes. At the current state of the art in FACS instrumentation, routine application of the FASS protocol is only feasible for glutamatergic synapses, because sorting of sufficient numbers of other synaptosome types (e.g. GABAergic,

cholinergic, or monoaminergic synaptosomes), would take far too much time due to their far lower abundance. In the future, improved FACS instrumentation may allow to circumvent this problem. Indeed, as flow cytometry allows for muti-parametric phenotyping of each analyzed particle separately, the FASS based separation of synapses by their neurotransmitter phenotype may only represent the beginning of a new era of investigations on brain tissue subcellular fractionations.

Materials and Methods

Animals

The generation and characterization of the VGLUT1^{VENUS} knock-in mouse line was published previously (Herzog *et al*, 2011). All animal experiments were performed in compliance with the European Communities Council Directive (86/809/EEC) regarding the care and use of animals for experimental procedures, the regulations of the Ministère de l'Agriculture et de la Forêt, Service Vétérinaire de la Santé et de la Protection Animale, France, and the guidelines for welfare of experimental animals issued by the State Government of Lower Saxony, Germany (comparable to NIH guidelines).

Preparation of S-synaptosomes for FASS

Our S-synaptosome preparation was adapted from two previously published protocols (Hebb & Whittaker, 1958; Huttner *et al*, 1983). Briefly, forebrains of one or two mice were homogenized in 4 ml of ice-cold homogenization buffer (0.32 M Sucrose, 4 mM HEPES pH 7.4, 1 μM PMSF, 1 μg/ml Aprotinin, 1 μg/ml Leupeptin) using a 5-ml glass-Teflon homogenizer with 12 gentle strokes. The homogenizer was then rinsed with additional 4 ml of homogenization buffer, and the combined 8 ml of homogenate (H) were centrifuged at 1000 *g* for 10 min at 4°C in an SS-34 rotor (Sorvall). The supernatant (S1) was removed from the pellet (P1) and centrifuged at 12,500 *g* for 15 min at 4°C in an SS-34 rotor. The supernatant (S2) was removed completely and the synaptosome-enriched pellet (P2) was resuspended in 1 ml of homogenization buffer. The P2 fraction was then layered on top of a two-step sucrose density gradient (5 ml of 1.2 M and 5 ml of 0.8 M sucrose, 4 mM HEPES, protease inhibitors as above). The gradient was centrifuged at 50,000 *g* for 70 min at 4°C in an SW-41Ti rotor (Beckman). S-synaptosomes were recovered at the interface of 0.8 and 1.2 M sucrose using a Pasteur pipette. The resulting fraction is referred to as sucrose gradient synaptosomes (S-synaptosomes). Methods for subcellular fractionations used during proteomics data validation (Fig 6) are detailed in the supplementary Data S1.

FACS instrumentation and FM4-64 triggering

The FACSAria-I (BD Biosciences) was operated using a 70 μm nozzle and the 488 nm laser line. For FM4-64 triggering the settings were as follows: 488 nm laser (area scaling 1.4, window extension 0.0, FSC area scaling 1.3), FSC (neutral density filter 1.0, 341 V), SSC (488/10 BP, 322 V), VGLUT1^{VENUS} (530/30 BP, 700 V), detection threshold for FM4-64, 800. Generally, flow cytometry data acquisition, analysis, and image preparation were carried out using the instrument software FACSDiva (BD Biosciences). Histogram overlays were produced using Adobe Photoshop (Adobe). Events with higher than WT VGLUT1^{VENUS} fluorescence intensity were sub-gated from the events of the single particle gate, and sorted fractions were re-analyzed by flow cytometry to control the success of sorting.

Fluorescence Activated Synaptosome Sorting

S-synaptosomes were stored on ice and protected from light. For flow cytometry analysis and sorting, S-synaptosomes were diluted in ice-cold PBS supplemented with protease inhibitors as above. Bulk red fluorescent labeling of all membranes for FM triggering was achieved by incubating 1.5 μg/ml of the lipophilic styryl dye FM4-64 with S-synaptosomes before sorting. Thresholding of detection was optimized using PBS/protease inhibitors/FM4-64 solution without S-synaptosomes. Samples were analyzed and sorted at event rates of 20,000–25,000 evt/s. A fresh suspension of synaptosomes was generated every 45–60 min. In FM triggering, single particles were gated in the 'small size' gate by excluding events that showed correlating high values for FSC area and SSC area (Fig 2). Events of the 'small size' gate were sub-gated according to VGLUT1^{VENUS} fluorescence intensity. Background fluorescence from WT S-synaptosomes was determined before each experiment (Fig 2). All sort experiments were carried out using the predefined 'purity' sort mask. For quality tests, sorted particles were reanalyzed by flow cytometry with identical instrument settings. For FM triggering, FM4-64 was added to the diluted FASS sample before reanalysis. For further FACS-independent analysis we implemented custom collection and concentration methods that are fully detailed in the supplemental methods.

SDS-PAGE and Western blotting

SDS-PAGE using Bis-Tris gradient gels (4–12% NuPAGE, Invitrogen) was carried out according to the manufacturer's recommendations. Colloidal Coomassie, silver staining and Western blotting was performed according to standard procedures. We used HRP-coupled secondary antibodies (Jackson Immuno Research), and visualized signals either on films by enhanced chemiluminescence (GE Healthcare) or on a G:Box iChemi CCD camera (Syngene) by SuperSignal West Femto chemiluminescence (ThermoScientific). Quantifications of Western blot signals were expressed as co-enrichment factor (CF) ± s.e.m. The CF represents the co-enrichment of a given protein relative to the enrichment of VGLUT1^{VENUS} in the sorted sample, compared with the unsorted sample. Significant pairwise differences were tested in a one-sided *t*-test (significance threshold of $P = 0.05$). Two markers (PSD95 and Synaptopodin1) that migrate close to VGLUT1^{venus} upon SDS-PAGE were quantified using EndophilinA1 as a reference. EndophilinA1 co-enriches very reliably with VGLUT1^{venus} (Fig 3A and B) and migrates faster than VGLUT1^{venus}. The following antibodies were used: Mouse monoclonal antibodies to GFP (1:1,000; Roche), PSD95 (6G6 1C9, 1:2,000; Abcam), PLP (3F4, 1:50; Greer & Lees, 2002), Synaptophysin (clone 7.2, 1:10,000), ClathrinLC (1:250) SNAP25 (1:1,000,000), Neuroligin-1 (clone 4C12, 1:8,000), and GluN1 (clone M68, 1:500) all from synaptic systems; polyclonal rabbit antisera to Synapsin (1:4,000), Rab3a (1:2,000), VAMP2 (1:4,000), Dynamin1 (1:2,000), Synaptopodin1 (1:500) all from synaptic systems; EndophilinA1, (1:2,000; Vinatier *et al*, 2006), VDAC (Rockland, 1:1,000), VIAAT (Chemicon, 1:250), GluA1 (Milipore, 1:1,000), VGLUT2 (57LP1, E. Herzog, Bordeaux,

France, unpublished), VAChT (1:4,000), SNAP23 (1:250), SNAP47 (1:1,000), SV2A (1:4,000), SV2B (1:4,000), Complexin-1/2 (1:1,000), GluA2 (1:500) all from Synaptic Systems, GluN2A and GluN2B (both Chemicon, 1:1,000), Tpd52 (1:250; Shehata *et al*, 2008), FXYD6 (1:2,000; Delprat *et al*, 2007); polyclonal guinea-pig antiserum to GLT1 (Chemicon, 1:20,000).

Histology, cell culture, and immunofluorescence microscopy

Preparation of brain sections of 10/15-week-old mice, continental primary hippocampal neuron cultures (DIV21-22), and immunofluorescence microscopy analyses thereof were performed as described previously (Herzog *et al*, 2011). The following antibodies were used: Mouse monoclonal antibodies to GFP (MAB3580, Millipore, 1:1,000), PSD95 (1:1,000; BD Transduction Labs), GAD67 (Millipore, 1:2,000), GAD65 (Millipore, 1:1,000), GFAP (1:500; Dako), MAP2 (Millipore, 1:2,000); rabbit polyclonal antisera to GFP (A6455, Invitrogen, 1:5,000), VIAAT (Synaptic Systems, 1:1,000), Tpd52 (1:300; Shehata *et al*, 2008), FXYD6 (1:2,000; Delprat *et al*, 2007).

Electron microscopy

For electron microscopy, sorted particles were collected onto Isopore™ filters as described above. The filters were then incubated with preheated synaptosome regeneration buffer (H_2O, 64 mM NaCl, 4 mM KCl, 0.8 mM $CaCl_2$, 0.8 mM $MgCl_2$, 8 mM Tris–HCl pH 7.4, 160 mM sucrose, 37°C) at room temperature for 20 min. Synaptosomes were immediately fixed in 2.5% glutaraldehyde in PBS for 30 min on ice. The filters were then washed, osmicated for 1 h (1% OsO_4), dehydrated through a graded series of ethanol, including a step of 1.5 h in 70% ethanol with 1.5% uranyl acetate, and embedded in Epon. Ultrathin sections (70 nm) were cut from three distinct locations of the filter membrane, and two sections of each location were contrasted with uranyl acetate and lead citrate, and imaged using a LEO912AB transmission electron microscope (Zeiss). Digital images were taken using a ProScan CCD camera (Proscan) and AnalySIS software (Olympus). Following export, images were processed and quantified manually using ImageJ software (Schneider *et al*, 2012). Imaging and image analysis and quantification were performed with the observer being blind to the experimental conditions. Pre-embedding immuno-electron microscopy of ultrathin sections using the anti-FXYD6 antibody was performed according to published procedures (Dobbertin *et al*, 2009).

Proteomics

Proteins were separated by SDS-PAGE. Lanes were excised from the colloidal Coomassie stained gel and cut into 24 bands. Each band was processed for in-gel tryptic digestion, including treatment with DTT and iodoacetamide. Tryptic peptides were extracted with formic acid and acetonitrile, and dried by vacuum centrifugation. Peptides were redissolved in 30 µl of 5% formic acid and analyzed by nanoLC-MS/MS using a LTQ XL Orbitrap (Thermo Fisher Scientific) coupled to an Agilent 1100 series LC-system (Agilent). Peptides were separated at a flow rate of 200–300 nl/min on a reverse-phase column (C18, Reprosil, Maisch). Elution of peptides was done with a 54 min gradient from 7 to 45% mobile phase B (80% acetonitrile, 0.15% formic acid). The instrument was operated with a spray voltage of 1.7 kV, heated capillary temperature was set to 150°C. Collision energy was 37.5%, activation was q = 0.25 and activation time was 30 ms. A 'top 5' (i.e. 5 MS/MS per MS scan) method was used in a data dependent acquisition mode. Survey scans (MS) were acquired from 350 to 1600 m/z in the Orbitrap with a resolution of 30,000 (at m/z 400) and the target for the automatic gain control (AGC) was set to 1×10^6. MS/MS fragmentation and detection was performed in linear ion trap. Single charged ions and ions with unrecognized charge states were excluded by the instrument method. Peak lists were searched against the NCBI RefSeq database using Mascot v.2.2 (Matrix Science) as the search engine. Mass accuracy was 10 ppm for the parent ion and 0.5 Da for the fragment ions. The data were filtered using a MASCOT $P < 0.05$. Peptides were constrained to be tryptic with a maximum of two missed cleavages. Carbamidomethylation of cysteines was considered a fixed modification, whereas oxidations of methionine and phosphorylation of serine, threonine, and tyrosine residues were considered as variable modifications. The results of two technical replicates were combined and analyzed using Scaffold (Proteome Software). Minimum protein identification and peptide identification thresholds were set to 95% and a minimum of two peptides was required. The fold change in normalized spectral counts between the two samples was computed. When proteins were identified in only one sample, the fold change was set to the maximum value of 10.

Supplementary information for this article is available online: www.emboj.embopress.org

Acknowledgements

We thank Mattia Aime, Fritz Benseler, Martin Doerre, Ines Eckhardt, Santiago Gonzalez, Elodie Kim Grellier, Klaus Hellmann, Markus Krohn, Tanja Leinert, Rainer Libal, Robert Otremba, Astrid Ohle, Vincent Pitard, Uwe Pleßmann Inga Schauenberg, Florian Schütte, Dayana Schwerdtfeger, Ivonne Thanhäuser, and Sally Wenger for their excellent technical assistance. We are grateful to Silvio Rizzoli, Ben Cooper (Göttingen, Germany), and Dominique Marie (Roscoff, France) for very helpful experimental advice, and to Käthi Geering (Lausanne, Switzerland), and Marjorie B. Lees (Waltham, MA, USA) for providing reagents. This work was supported by the European Union (EUROSPIN and SynSys, to N.B.), the Max Planck Society (to N.B.), the German Research Foundation (grant GRK521 to N.B. and F.V.), and the Agence Nationale de la Recherche (ANR-12-JSV4-0005-01 VGLUT-IQ and ANR-10-LABX-43 BRAIN to E.H.). C.B. was a student of the Molecular Biology Ph.D. Program, the International Max Planck Research School for Molecular Biology, and the Göttingen Graduate School for Neurosciences, Biophysics, and Molecular Biosciences (GGNB) at the Georg August University Göttingen (German Research Foundation grant GSC 226/1).

Author contributions

CB performed and analyzed most experiments and wrote the paper; MG contributed to the design, execution and analysis of the proteomics experiments; EL performed a subset of FASS and Western blot experiments; SPW performed the transcriptomics/proteomics meta-analysis; VB performed and analyzed immuno-electron microscopy experiments; SB performed some biochemical experiments; FV supervised the electron microscopy on synaptosomes; LL generated supplementary Fig S2; JAB provided reagents for and expertise on tpd52 protein; HU supervised the proteomics experiments; OJ supervised the proteomics experiments; NB supervised the project and wrote the paper; EH

performed experiments, analyzed data, supervised the project, and wrote the paper; BC provided technical supervision over the electron microscopy on synaptosomes.

Conflict of interest

The authors declare that they have no conflict of interest.

References

Abul-Husn NS, Devi LA (2006) Neuroproteomics of the synapse and drug addiction. *J Pharmacol Exp Ther* 318: 461 – 468

Al-Hallaq RA, Yasuda RP, Wolfe BB (2001) Enrichment of *N*-methyl-D-aspartate NR1 splice variants and synaptic proteins in rat postsynaptic densities. *J Neurochem* 77: 110 – 119

Bai F, Witzmann FA (2007) Synaptosome proteomics. *Subcell Biochem* 43: 77 – 98

Bajjalieh SM, Frantz GD, Weimann JM, McConnell SK, Scheller RH (1994) Differential expression of synaptic vesicle protein 2 (SV2) isoforms. *J Neurosci* 14: 5223 – 5235

Bard L, Groc L (2011) Glutamate receptor dynamics and protein interaction: lessons from the NMDA receptor. *Mol Cell Neurosci* 48: 298 – 307

Baudouin SJ, Gaudias J, Gerharz S, Hatstatt L, Zhou K, Punnakkal P, Tanaka KF, Spooren W, Hen R, De Zeeuw CI, Vogt K, Scheiffele P (2012) Shared synaptic pathophysiology in syndromic and nonsyndromic rodent models of autism. *Science* 338: 128 – 132

Boutros R, Fanayan S, Shehata M, Byrne JA (2004) The tumor protein D52 family: many pieces, many puzzles. *Biochem Biophys Res Commun* 325: 1115 – 1121

Boyken J, Grønborg M, Riedel D, Urlaub H, Jahn R, Chua JJE (2013) Molecular profiling of synaptic vesicle docking sites reveals novel proteins but few differences between glutamatergic and GABAergic synapses. *Neuron* 78: 285 – 297

Bragina L, Candiracci C, Barbaresi P, Giovedi S, Benfenati F, Conti F (2007) Heterogeneity of glutamatergic and GABAergic release machinery in cerebral cortex. *Neuroscience* 146: 1829 – 1840

Brose N (2008) For better or for worse: complexins regulate SNARE function and vesicle fusion. *Traffic* 9: 1403 – 1413

Burré J, Volknandt W (2007) The synaptic vesicle proteome. *J Neurochem* 101: 1448 – 1462

Byrne JA, Mattei M-G, Basset P (1996) Definition of the tumor protein D52 (TPD52) gene family through cloning of D52 homologues in human (hD53) and mouse (mD52). *Genomics* 35: 523 – 532

Cahoy JD, Emery B, Kaushal A, Foo LC, Zamanian JL, Christopherson KS, Xing Y, Lubischer JL, Krieg PA, Krupenko SA, Thompson WJ, Barres BA (2008) A transcriptome database for astrocytes, neurons, and oligodendrocytes: a new resource for understanding brain development and function. *J Neurosci* 28: 264 – 278

Cheng D, Hoogenraad CC, Rush J, Ramm E, Schlager MA, Duong DM, Xu P, Wijayawardana SR, Hanfelt J, Nakagawa T, Sheng M, Peng J (2006) Relative and absolute quantification of postsynaptic density proteome isolated from rat forebrain and cerebellum. *Mol Cell Proteomics* 5: 1158 – 1170

Chew CS, Chen X, Zhang H, Berg EA, Zhang H (2008) Calcium/calmodulin-dependent phosphorylation of tumor protein D52 on serine residue 136 may be mediated by CAMK2 6. *Am J Physiol Gastrointest Liver Physiol* 295: G1159 – G1172

Chua JJE, Kindler S, Boyken J, Jahn R (2010) The architecture of an excitatory synapse. *J Cell Sci* 123: 819 – 823

Collins MO, Husi H, Yu L, Brandon JM, Anderson CNG, Blackstock WP, Choudhary JS, Grant SGN (2006) Molecular characterization and comparison of the components and multiprotein complexes in the postsynaptic proteome. *J Neurochem* 97(Suppl. 1): 16 – 23

Cotman CW, Matthews DA (1971) Synaptic plasma membranes from rat brain synaptosomes: isolation and partial characterization. *Biochim Biophys Acta* 249: 380 – 394

De Gois S, Jeanclos E, Morris M, Grewal S, Varoqui H, Erickson JD (2006) Identification of endophilins 1 and 3 as selective binding partners for VGLUT1 and their co-localization in neocortical glutamatergic synapses: implications for vesicular glutamate transporter trafficking and excitatory vesicle formation. *Cell Mol Neurobiol* 26: 679 – 693

Delprat B, Schaer D, Roy S, Wang J, Puel J-L, Geering K (2007) FXYD6 is a novel regulator of Na,K-ATPase expressed in the inner ear. *J Biol Chem* 282: 7450 – 7456

Dobbertin A, Hrabovska A, Dembele K, Camp S, Taylor P, Krejci E, Bernard V (2009) Targeting of acetylcholinesterase in neurons *in vivo*: a dual processing function for the proline-rich membrane anchor subunit and the attachment domain on the catalytic subunit. *J Neurosci* 29: 4519 – 4530

Docherty M, Bradford HF, Wu JY (1987) Co-release of glutamate and aspartate from cholinergic and GABAergic synaptosomes. *Nature* 330: 64 – 66

Dodd P, Hardy JA, Oakley AE, Strong AJ (1981) Synaptosomes prepared from fresh human cerebral cortex; morphology, respiration and release of transmitter amino acids. *Brain Res* 224: 419 – 425

Fremeau RT, Voglmaier S, Seal RP, Edwards RH (2004) VGLUTs define subsets of excitatory neurons and suggest novel roles for glutamate. *Trends Neurosci* 27: 98 – 103

Gardoni F, Picconi B, Ghiglieri V, Polli F, Bagetta V, Bernardi G, Cattabeni F, Di Luca M, Calabresi P (2006) A critical interaction between NR2B and MAGUK in L-DOPA induced dyskinesia. *J Neurosci* 26: 2914 – 2922

Garty H, Karlish SJD (2006) Role of FXYD proteins in ion transport. *Annu Rev Physiol* 68: 431 – 459

Geering K (2006) FXYD proteins: new regulators of Na-K-ATPase. *Am J Physiol Renal Physiol* 290: F241 – F250

Gray EG, Whittaker VP (1962) The isolation of nerve endings from brain: an electron microscopic study of cell fragments derived by homogenization and centrifugation. *J Anat* 96: 79 – 88

Greer JM, Lees MB (2002) Myelin proteolipid protein–the first 50 years. *Int J Biochem Cell Biol* 34: 211 – 215

Groblewski GE, Yoshida M, Yao H, Williams JA, Ernst SA (1999) Immunolocalization of CRHSP28 in exocrine digestive glands and gastrointestinal tissues of the rat. *Am J Physiol* 276: G219 – G226

Grønborg M, Pavlos NJ, Brunk I, Chua JJE, Munster-Wandowski A, Riedel D, Ahnert-Hilger G, Urlaub H, Jahn R (2010) Quantitative comparison of glutamatergic and GABAergic synaptic vesicles unveils selectivity for few proteins including MAL2, a novel synaptic vesicle protein. *J Neurosci* 30: 2 – 12

Gylys KH, Fein JA, Yang F, Cole GM (2004) Enrichment of presynaptic and postsynaptic markers by size-based gating analysis of synaptosome preparations from rat and human cortex. *Cytometry A* 60: 90 – 96

Hebb CO, Whittaker VP (1958) Intracellular distributions of acetylcholine and choline acetylase. *J Physiol (Lond)* 142: 187 – 196

Henn FA, Anderson DJ, Rustad DG (1976) Glial contamination of synaptosomal fractions. *Brain Res* 101: 341 – 344

Herzog E, Nadrigny F, Silm K, Biesemann C, Helling I, Bersot T, Steffens H, Schwartzmann R, Nägerl UV, Mestikawy El S, Rhee J, Kirchhoff F, Brose N (2011) *In vivo* imaging of intersynaptic vesicle exchange using VGLUT1Venus knock-in mice. *J Neurosci* 31: 15544 – 15559

Hippenmeyer S, Kramer I, Arber S (2004) Control of neuronal phenotype: what targets tell the cell bodies. *Trends Neurosci* 27: 482 – 488

Holt M, Varoqueaux F, Wiederhold K, Takamori S, Urlaub H, Fasshauer D & Jahn R (2006) Identification of SNAP-47, a novel Qbc-SNARE with ubiquitous expression. *J Biol Chem* 281: 17076 – 17083

Hoon M, Soykan T, Falkenburger B, Hammer M, Patrizi A, Schmidt K-F, Sassoè-Pognetto M, Löwel S, Moser T, Taschenberger H, Brose N, Varoqueaux F (2011) Neuroligin-4 is localized to glycinergic postsynapses and regulates inhibition in the retina. *Proc Natl Acad Sci U S A* 108: 3053 – 3058

Huttner WB, Schiebler W, Greengard P, De Camilli P (1983) Synapsin I (protein I), a nerve terminal-specific phosphoprotein. III. Its association with synaptic vesicles studied in a highly purified synaptic vesicle preparation. *J Cell Biol* 96: 1374 – 1388

Imai Y, Ibata I, Ito D, Ohsawa K, Kohsaka S (1996) A novel gene iba1 in the major histocompatibility complex class III region encoding an EF hand protein expressed in a monocytic lineage. *Biochem Biophys Res Commun* 224: 855 – 862

Kadowaki K, Sugimoto K, Yamaguchi F, Song T, Watanabe Y, Singh K, Tokuda M (2004) Phosphohippolin expression in the rat central nervous system. *Brain Res Mol Brain Res* 125: 105 – 112

Krueger DD, Tuffy LP, Papadopoulos T, Brose N (2012) The role of neurexins and neuroligins in the formation, maturation, and function of vertebrate synapses. *Curr Opin Neurobiol* 22: 412 – 422

Masson J, Sagné C, Hamon M, Mestikawy El S (1999) Neurotransmitter transporters in the central nervous system. *Pharmacol Rev* 51: 439 – 464

Milnerwood AJ, Gladding CM, Pouladi MA, Kaufman AM, Hines RM, Boyd JD, Ko RWY, Vasuta OC, Graham RK, Hayden MR, Murphy TH, Raymond LA (2010) Early increase in extrasynaptic NMDA receptor signaling and expression contributes to phenotype onset in Huntington's disease mice. *Neuron* 65: 178 – 190

Morciano M, Beckhaus T, Karas M, Zimmermann H, Volknandt W (2009) The proteome of the presynaptic active zone: from docked synaptic vesicles to adhesion molecules and maxi-channels. *J Neurochem* 108: 662 – 675

Okabe S (2007) Molecular anatomy of the postsynaptic density. *Mol Cell Neurosci* 34: 503 – 518

Oldham MC, Konopka G, Iwamoto K, Langfelder P, Kato T, Horvath S, Geschwind DH (2008) Functional organization of the transcriptome in human brain. *Nat Neurosci* 11: 1271 – 1282

Parente JA, Goldenring JR, Petropoulos AC, Hellman U, Chew CS (1996) Purification, cloning, and expression of a novel, endogenous, calcium-sensitive, 28-kDa phosphoprotein. *J Biol Chem* 271: 20096 – 20101

Pines G, Danbolt NC, Bjørås M, Zhang Y, Bendahan A, Eide L, Koepsell H, Storm-Mathisen J, Seeberg E, Kanner BI (1992) Cloning and expression of a rat brain L-glutamate transporter. *Nature* 360: 464 – 467

Schneider CA, Rasband WS, Eliceiri KW (2012) NIH Image to ImageJ: 25 years of image analysis. *Nature Methods* 9: 671 – 675

Shehata M, Bièche I, Boutros R, Weidenhofer J, Fanayan S, Spalding L, Zeps N, Byth K, Bright RK, Lidereau R, Byrne JA (2008) Nonredundant functions for tumor protein D52-like proteins support specific targeting of TPD52. *Clin Cancer Res* 14: 5050 – 5060

Shepherd GM, Harris KM (1998) Three-dimensional structure and composition of CA3–>CA1 axons in rat hippocampal slices: implications for presynaptic connectivity and compartmentalization. *J Neurosci* 18: 8300 – 8310

Shoshan-Barmatz V, De Pinto V, Zweckstetter M, Raviv Z, Keinan N, Arbel N (2010) VDAC, a multi-functional mitochondrial protein regulating cell life and death. *Mol Aspects Med* 31: 227 – 285

Sokolow S, Luu SH, Nandy K, Miller CA, Vinters HV, Poon WW, Gylys KH (2012) Preferential accumulation of amyloid-beta in presynaptic glutamatergic terminals (VGluT1 and VGluT2) in Alzheimer's disease cortex. *Neurobiol Dis* 45: 381 – 387

Song JY, Ichtchenko K, Südhof TC, Brose N (1999) Neuroligin 1 is a postsynaptic cell-adhesion molecule of excitatory synapses. *Proc Natl Acad Sci U S A* 96: 1100 – 1105

Südhof TC, Rothman JE (2009) Membrane fusion: grappling with SNARE and SM proteins. *Science* 323: 474 – 477

Takahashi S, Yamamoto H, Matsuda Z, Ogawa M, Yagyu K, Taniguchi T, Miyata T, Kaba H, Higuchi T, Okutani F (1995) Identification of two highly homologous presynaptic proteins distinctly localized at the dendritic and somatic synapses. *FEBS Lett* 368: 455 – 460

Takamori S (2006) VGLUTs: 'exciting' times for glutamatergic research? *Neurosci Res* 55: 343 – 351

Takamori S, Holt M, Stenius K, Lemke EA, Grønborg M, Riedel D, Urlaub H, Schenck S, Brügger B, Ringler P, Müller SA, Rammner B, Gräter F, Hub JS, De Groot BL, Mieskes G, Moriyama Y, Klingauf J, Grubmüller H, Heuser J *et al* (2006) Molecular anatomy of a trafficking organelle. *Cell* 127: 831 – 846

Thomas CG, Miller AJ, Westbrook GL (2006) Synaptic and extrasynaptic NMDA receptor NR2 subunits in cultured hippocampal neurons. *J Neurophysiol* 95: 1727 – 1734

Tribl F, Marcus K, Bringmann G, Meyer HE, Gerlach M, Riederer P (2006) Proteomics of the human brain: sub-proteomes might hold the key to handle brain complexity. *J Neural Transm* 113: 1041 – 1054

Varoqueaux F, Jamain S, Brose N (2004) Neuroligin 2 is exclusively localized to inhibitory synapses. *Eur J Cell Biol* 83: 449 – 456

Vinatier J, Herzog E, Plamont M-A, Wojcik SM, Schmidt A, Brose N, Daviet L, Mestikawy El S, Giros B (2006) Interaction between the vesicular glutamate transporter type 1 and endophilin A1, a protein essential for endocytosis. *J Neurochem* 97: 1111 – 1125

Voglmaier SM, Kam K, Yang H, Fortin DL, Hua Z, Nicoll RA, Edwards RH (2006) Distinct endocytic pathways control the rate and extent of synaptic vesicle protein recycling. *Neuron* 51: 71 – 84

Whittaker VP (1959) The isolation and characterization of acetylcholine-containing particles from brain. *Biochem J* 72: 694 – 706

Whittaker VP (1993) Thirty years of synaptosome research. *J Neurocytol* 22: 735 – 742

Whittaker VP, Michaelson IA, Kirkland RJ (1964) The separation of synaptic vesicles from nerve-ending particles ('synaptosomes'). *Biochem J* 90: 293 – 303

Wilson SH, Bailey AM, Nourse CR, Mattei MG, Byrne JA (2001) Identification of MAL2, a novel member of the mal proteolipid family, though interactions with TPD52-like proteins in the yeast two-hybrid system. *Genomics* 76: 81 – 88

Wolf ME, Kapatos G (1989a) Flow cytometric analysis of rat striatal nerve terminals. *J Neurosci* 9: 94 – 105

Wolf ME, Kapatos G (1989b) Flow cytometric analysis and isolation of permeabilized dopamine nerve terminals from rat striatum. *J Neurosci* 9: 106 – 114

Yamada M, Saisu H, Ishizuka T, Takahashi H, Abe T (1999) Immunohistochemical distribution of the two isoforms of synaphin/complexin involved in neurotransmitter release: localization at the distinct central nervous system regions and synaptic types. *Neuroscience* 93: 7 – 18

Yamaguchi F, Yamaguchi K, Tai Y, Sugimoto K, Tokuda M (2001) Molecular cloning and characterization of a novel phospholemman-like protein from rat hippocampus. *Brain Res Mol Brain Res* 86: 189 – 192

